## **Silence Localization**

Alireza Chamanzar and Pulkit Grover

Abstract—We present a novel algorithm for non-invasive localization of regions of "silence" in the brain. "Silences" are sources in the brain without any electrical activity due to the ischemic conditions or lesions in stroke, traumatic brain injuries (TBIs) and hemorrhages. We aim to turn the widely used electroencephalography (EEG) systems into silence detectors. Our algorithm, in a nutshell, estimates the silence region by determining the contribution of each source (dipole) in the recorded signals and detects the sources with a reduced contribution as silences in the brain. In simulations on realhead MRI models, our algorithm detects different sizes of silent regions, ranging from the smallest ones (single-source silence) to the large ones, and it reduces bias by a factor of  $\sim$ 4 over classical source localization algorithms such as multiple signal classification approach (MUSIC) and minimum norm estimation (MNE), appropriately modified for recovering silences.

#### I. INTRODUCTION

In this paper, we introduce a novel method for the detection of regions of "silence" in the brain, using non-invasive electroencephalography (EEG) signals, where "silence" is defined as a source in the brain (dipole) without any electrical activity. Based on this definition, a region of silence models an ischemic tissue, a dead part of brain tissue, or a lesion which can be formed in a wide variety of situations, e.g., traumatic brain injuries (TBI), and ischemic stroke. It also approximately models (for a small time frame of a few tens of seconds) cortical spreading depolarizations (CSDs), which are waves of neural silence that travel very slowly on the brain surface [1], [2], [3], [4]. Commonly, brain silences are detected using classical imaging techniques such as magnetic resonance imaging (MRI) or computed tomography (CT) [1], [5], [6]. However, patients cannot be put under an MRI or CT scanner when they arrive in emergency situations to the clinic.

EEG is a non-invasive recording technique which is widely used, even in intensive care units (ICUs), for continuous or short-term recordings. It has easy and fast recording preparation, it is portable, and does not have the limitations of MRI, such as the inability to record from patients with emergency situations, or patients with metallic objects in their body [7]. This motivates us to ask this question: is it possible to detect and localize brain silences using portable and non-invasive EEG recordings? EEG signals are noisy and spatially low-pass filtered representation of electrical activities in the brain [8], [9]. This makes silence localization

difficult. In this paper, we aim to find a solution to this problem.

#### A. Forward model

Electrical activities of neurons in the brain produce electrical potentials on the scalp. Neurons or groups of neurons can be modeled as current dipoles [9]. To simulate the EEG signals on the scalp, we use a linear transformation to map the electrical activity of brain sources (dipoles) on to the scalp. This linear transformation is a forward-field approximation to Maxwell's equations and is called the "forward model" [10], which can be written in the form of a matrix for discretized brain space.

In this paper an open source MRI database (OASIS¹) is used to obtain real head models, based on which the forward model is extracted using Boundary Element Method (BEM) volume conduction model with conductivity ratios of 1, 0.067, 5, 1 for scalp, skull, cerebrospinal fluid (CSF), and brain as it is used in [11]. We choose MRI image set of a healthy subject (OASIS34: 51 years old) and use *FreeSurfer*² to process this MRI image and extract different layers of the head. Next, using *FieldTrip* [12], a freely available MATLAB toolbox, we generate the forward matrix, which has the number of rows equal to the number of EEG sensors on the scalp, and the number of columns equal to the number of electrical sources (dipole sources normal to the surface of tessellated cortex and placed at the vertices [9]) in the brain. This is called forward matrix ("A" in (1)).

#### B. Problem statement

The linear forward model can be written as below:

$$\mathbf{M}_{n\times t} = \mathbf{A}_{n\times p} \mathbf{S}_{p\times t} + \boldsymbol{\varepsilon}_{n\times t}, \tag{1}$$

where **A** is the forward matrix, **M** is the matrix of observations where each row represents the signal of one sensor across time, **S** is the matrix of source signals,  $\boldsymbol{\varepsilon} = [\varepsilon_1, \varepsilon_2, \cdots, \varepsilon_t]$  is the measurement noise, t is the number of time points, p is the number of cortical sources, and n is the number of EEG sensors placed in a uniform low-density grid similar to the one used in [3].

Objective: Given M and A, localize the "silence region" in S.

Source localization algorithms often assume that there is a source that is persistent across time or trials that has activity larger than that at other locations. Here, instead, we are interested in a persistent *lack* of activity.

We make the following assumptions: (i) Without loss of generality, we assume that the columns of A are normalized [13]; (ii) A is known, and M has been recorded; (iii)  $\varepsilon$ 

<sup>\*</sup>This research was supported in part by the CMU CIT Incubation Award, NSF WiFiUS program, and a CMU BrainHUB award.

<sup>\*</sup>We thank Marlene Behrmann, Sanghamitra Dutta, Praveen Venkatesh, and Chaitanya Goswami for helpful discussions.

The authors are at Carnegie Mellon University {achamanz, pgrover}@andrew.cmu.edu

<sup>&</sup>lt;sup>1</sup>http://www.oasis-brains.org

<sup>&</sup>lt;sup>2</sup>https://surfer.nmr.mgh.harvard.edu

is additive white Gaussian noise whose elements are assumed to be independent and identically distributed (iid) across time and space, i.e., at each time, the covariance matrix is  $\mathbf{C} = \sigma_n^2 \mathbf{I}_{n \times n}$ . We assume that  $\sigma_n^2$  is known ( $\sigma_n^2$ ); (iv)  $\mathbf{S}$  is a random matrix with elements are drawn from an iid Gaussian distribution, except for the k rows that correspond to the "silence" region which are rows of all zeros; (v) The number of active sources, p - k, is greater than the number of silences, k; (vi) Silent sources are contiguous; and (vii) t is large enough so that  $\mathbf{S}$  contains activities in all parts of the cortex, except in silent regions. Assumption (iv) is made for simplicity, and might strike as being unrealistic. In Section III we discuss how this can be relaxed.

In Section II we introduce our proposed silence localization algorithm, in addition to the two classical source localization methods – MUSIC and MNE – which are modified appropriately for silence localization. In Section III, we present the results of silence localization using our algorithm and compare the performance of our proposed algorithm with the two other algorithms. Finally, we discuss the limitations of the proposed algorithm and some possible directions for future work.

#### II. ALGORITHM

The major challenges in this inverse problem are: (1) this problem is severely underdetermined, since  $p \gg n$ , which is a common issue in source localization problems. Existing algorithms tackle this issue with different approaches such as regularization methods and exploiting prior knowledge about sources; (2) the source in this problem is not sparse, i.e., the number of active sources is greater than the number of silences, In the next section it is shown how this results in the failure of existing source-localization algorithms.

## A. Proposed algorithm

In our algorithm, we measure the contribution of each source (dipole) in the observation data (M) and detect the sources with lack of such contribution as silences in the brain. Following are the steps of our algorithm:

1) Cross-correlation: The linear model in (1) can be rewritten in this form:

$$\mathbf{m}_i = \sum_{j=1}^p \mathbf{a}_j s_{ji} + \boldsymbol{\varepsilon}_i, \quad \forall \ i = \{1, 2, \dots t\},$$
 (2)

where  $s_{ji}$  is the  $j^{th}$  element of the  $i^{th}$  column in  $\mathbf{S}$ ,  $\mathbf{M} = [\mathbf{m}_1, \cdots, \mathbf{m}_t] \in \mathbb{R}^{n \times t}$ ,  $\mathbf{S} = [\mathbf{s}_1, \cdots, \mathbf{s}_t] \in \mathbb{R}^{p \times t}$ ,  $\mathbf{A} = [\mathbf{a}_1, \cdots, \mathbf{a}_p] \in \mathbb{R}^{n \times p}$ , and  $\boldsymbol{\varepsilon} = [\boldsymbol{\varepsilon}_1, \cdots, \boldsymbol{\varepsilon}_t] \in \mathbb{R}^{n \times t}$ .

Based on (2), each observation vector  $\mathbf{m}_i$  is a linear combination of columns of the forward matrix  $\mathbf{A}$  with weights equal to the corresponding source values. However, in the presence of silences, those columns of  $\mathbf{A}$  at silence locations will never contribute to this summation. Therefore, we calculate the cross-correlation coefficient " $\mu_{qi}$ ", which measures this contribution, defined as follows:

$$\mu_{qi} = \mathbf{a}_q^T \mathbf{m}_i = \sum_{j=1}^p \mathbf{a}_q^T \mathbf{a}_j s_{ji} + \mathbf{a}_q^T \boldsymbol{\varepsilon}_i, \quad \forall \ q = \{1, 2, \dots p\},$$

$$\forall \ i = \{1, 2, \dots t\}.$$
(3)

2) Variance reduction estimation: In this step, we estimate the variance of correlation coefficients which are calculated in the first step. Based on (3) we have:

$$Var(\boldsymbol{\mu}_{qi}) = Var(\boldsymbol{\Sigma}_{j=1}^{p} \mathbf{a}_{q}^{T} \mathbf{a}_{j} s_{ji} + \mathbf{a}_{q}^{T} \boldsymbol{\varepsilon}_{i})$$

$$\stackrel{\text{(a)}}{=} Var(\boldsymbol{\Sigma}_{j=1}^{p} \mathbf{a}_{q}^{T} \mathbf{a}_{j} s_{ji}) + Var(\mathbf{a}_{q}^{T} \boldsymbol{\varepsilon}_{i})$$

$$\stackrel{\text{(b)}}{=} \boldsymbol{\Sigma}_{j=1}^{p} Var(\mathbf{a}_{q}^{T} \mathbf{a}_{j} s_{ji}) + Var(\mathbf{a}_{q}^{T} \boldsymbol{\varepsilon}_{i})$$

$$\stackrel{\text{(c)}}{=} \boldsymbol{\Sigma}_{j=1}^{p} (\mathbf{a}_{q}^{T} \mathbf{a}_{j})^{2} \sigma_{s}^{2} + (\|\mathbf{a}_{q}\|_{2}^{2} \sigma_{n}^{2})$$

$$\stackrel{\text{(d)}}{=} \boldsymbol{\Sigma}_{j=1}^{p} (\mathbf{a}_{q}^{T} \mathbf{a}_{j})^{2} \sigma_{s}^{2} + \sigma_{n}^{2},$$

$$\stackrel{\text{(d)}}{=} \boldsymbol{\Sigma}_{j=1}^{p} (\mathbf{a}_{q}^{T} \mathbf{a}_{j})^{2} \sigma_{s}^{2} + \sigma_{n}^{2},$$

where  $I_s$  is the indices of silences ( $I_s = \{j | s_{ji} = 0, \forall i = 1, 2, \cdots t\}$ ). In (4), the equation (a) and (b) hold because of the independence assumption of noise and sources, (c) holds because of identical distribution assumptions in S and  $\varepsilon$ , and (d) holds because the columns of  $\mathbf{A}$  are normalized. On the other hand, we can estimate these variances numerically using the time samples of  $\mu_{qi}$ , as follows:

$$\widehat{Var}(\mu_{qi}) = \frac{1}{t-1} \sum_{i=1}^{t} (\mu_{qi})^2,$$
 (5)

where t-1 is used instead of t for unbiasedness of the estimator. (4) shows how silences cause variance reduction at each source index. We build our silence detector based on this variance reduction. However, a normalization step is required to compare the reduction ratios rather than absolute reductions corresponding to each source:

$$Var(\boldsymbol{\mu}_{qi}) = \sum_{\substack{j=1 \ j \notin I_s}}^{p} (\mathbf{a}_q^T \mathbf{a}_j)^2 \sigma_s^2 + \sigma_n^2$$

$$= \sum_{j=1}^{p} (\mathbf{a}_q^T \mathbf{a}_j)^2 \sigma_s^2 - \sum_{j \in I_s} (\mathbf{a}_q^T \mathbf{a}_j)^2 \sigma_s^2 + \sigma_n^2,$$
(6)

$$\beta_q = \frac{\widehat{Var}(\mu_{qi}) - \sigma_n^2}{\sum_{i=1}^p (\mathbf{a}_q^T \mathbf{a}_j)^2} \approx \sigma_s^2 - \frac{\Delta Var(\mu_{qi})}{\sum_{i=1}^p (\mathbf{a}_q^T \mathbf{a}_j)^2} \sigma_s^2, \tag{7}$$

where  $\Delta Var(\mu_{qi}) = \Sigma_{j \in I_s}(\mathbf{a}_q^T\mathbf{a}_j)^2$ . In (7), the coefficient of  $\sigma_s^2$  in the second term is a value in the range [0,1], which captures the percentage of reduction in variance because of silences. Therefore,  $\beta_q$  is a reasonable measure of silences.

- 3) Estimation of the number of silences (k): In this step, we find an approximation of the number of silences based on the  $\beta_q$  values we found in the previous step. First, the  $\beta_q$  values are sorted in the ascending order and normalized ( $\tilde{\beta}_q$ ). Then, a "knee" point is defined in the curve of ( $\tilde{\beta}_q$ ) vs. q, where there is a sudden decrease in the growth rate of  $\tilde{\beta}_q$  as shown in Fig. 1a [14], [15]. To find this knee point, the closest point to the origin in the curve of  $1 \tilde{\beta}_q$  vs. q is found  $(q = \hat{k} + 1)$ , where  $\hat{k}$  is an estimation for k (see Fig. 1b).
- 4) Grouping sources based on their orientations: In this step, we group the sources based on the orientation of their corresponding columns in A, i.e., we assign a subset of source indices to each source with index i, whose corresponding columns  $a_i$  lie at nearby angles:

$$G_i = \{j | (\mathbf{a}_i^T \mathbf{a}_i)^2 = \cos^2(\theta_{ij}) \ge \gamma\}, \quad i = 1, 2, \dots p$$
 (8)

where  $\gamma$  is a threshold with value in [0,1] which specifies how small these angles  $\theta_{ij}$  should be, for each group. This

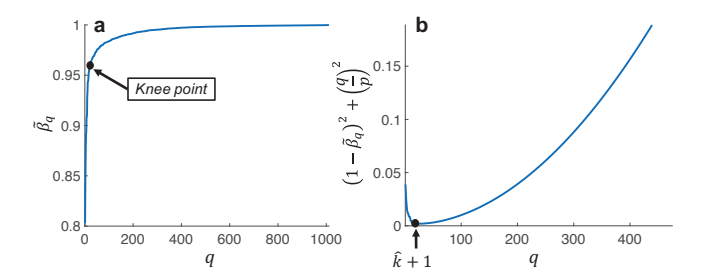


Fig. 1. Estimation of number of silences (k): a)  $\tilde{\beta}_q$ , which is the sorted  $\beta_q$  in an ascending order. This curve shows the variance reduction of correlation coefficients  $(\mu_{qi})$  because of silences. In this curve, a "Knee" point is defined where there is a sudden decrease in the growth rate of  $\tilde{\beta}_q$ ; b) Distance of points from the origin in the  $1-\tilde{\beta}_q$  vs. q curve. The index of point  $(\hat{k})$  with the minimum distance from the origin is an estimation of k.

grouping step helps in reducing the error in silence localization because **A** has highly correlated columns. However, if a very small  $\gamma$  is used, spatial resolution is lowered. Therefore, there is a trade-off in choosing  $\gamma$ .

- 5) Scoring Groups based on variance reduction: We use the  $\beta_q$  values in step 2 to assign a score to each group of sources. This score is simply the average of  $\beta_q$  for the members of each group  $(\bar{\beta}_{G_i} = \frac{1}{|G_i|} \Sigma_{q=1}^{|G_i|} \beta_q)$ , where  $|G_i|$  is the cardinality of  $G_i$ ). The smaller the score  $\bar{\beta}_{G_i}$  is, the higher is the chance that the corresponding group contains silence(s). Therefore we sort the groups in the ascending order based on their scores and choose the top  $\hat{k}$  groups, where  $\hat{k}$  is the estimated number of silences. This gives us more than or equal to  $\hat{k}$  indices, since each group may have more than one member.
- 6) Detecting region of silence: Based on the extracted source indices in the previous step, we try to exploit the knowledge that the region of silence is contiguous. To do so, we calculate the geometric center of the selected source indices and choose the  $2\hat{k}$  sources with the shortest distance to this central point. Now we sort these  $2\hat{k}$  sources based on their  $\beta_q$  values and choose the  $\hat{k}$  sources with the smallest  $\beta_q$  as the detected silences. This last step of our algorithm guarantees that the selected silences lie close to each other and form a region of silence and rejects the isolated silences that are selected in step 4.

### B. Modified minimum norm estimation (MNE)

In this paper, in order to compare the performance of our algorithm with classical source localization methods, we modify some of the commonly used algorithms to adopt them to the silence localization problem and to be able to perform the comparison. One of the most commonly used source localization method is the minimum norm estimation (MNE). In this algorithm, an estimation of the matrix of source signals is obtained through a regularization method:

$$\hat{\mathbf{S}} = \underset{\mathbf{S}}{\operatorname{argmin}} \|\mathbf{M} - \mathbf{A}\mathbf{S}\|_F^2 + \lambda \|\mathbf{S}\|_F^2, \tag{9}$$

This has the following closed form solution, where  $\lambda$  is obtained using the L-curve in this paper:

$$\hat{\mathbf{S}} = \mathbf{A}^T (\mathbf{A} \mathbf{A}^T + \lambda \mathbf{I}_{n \times n})^{-1} \mathbf{M}, \tag{10}$$

Based on this estimated source matrix ( $\hat{\mathbf{S}}$ ), we localize the silences as follows: (i) Start with  $\hat{k} = \frac{p}{2}$ ; (ii) Calculate the square of the elements in  $\hat{\mathbf{S}}$  ( $\hat{\mathbf{s}}_{ij}^2$ ,  $\forall$   $i = \{1, 2, \cdots p\}$ ,  $\forall$   $j = \{1, 2, \cdots t\}$ ) to compare the source powers; (iii) For each time point j, sort the  $\hat{\mathbf{s}}_{ij}^2$  in the ascending order and choose the first  $\hat{k}$  corresponding sources ( $I_{MNE}$ ), which are the sources with the minimum power at time j; (iv) Based on the repetition of sources in  $I_{MNE}$  calculate a histogram ( $hist_{MNE}$ ). Then sort this histogram in the descending order (the source with the largest population first); (v) Use a similar method to the one explained in Section II-A, step 3, to find an estimation of the number of silences ( $\hat{k}$ ). The knee point of sorted  $hist_{MNE}$  vs. source index curve is used to estimate k; (vi) Repeat step 4 to 6 in Section II-A. The only difference is that we use the  $hist_{MNE}$  instead of  $\beta_q$  for this modified MNE algorithm.

# C. Modified multiple signal classification approach (MU-SIC)

In addition to the MNE, multiple signal classification approach (MUSIC) is another source localization algorithm. which searches for each source sequential, rather than finding all sources at the same time based on the whole observation matrix M, since we can search for inactive sources. The main idea of MUSIC is using singular value decomposition (SVD) of observation matrix  $\mathbf{M} (= \mathbf{U} \Sigma \mathbf{V}^T)$  to reconstruct an orthogonal projection to the noise space of M to check which sources have minimum contributions in the recordings [10]. We modify this algorithm to adapt it to the silence localization problem. We select the left singular vectors (columns of U) which correspond to the large singular values up to 90% of the total energy of the matrix  $(\sum_{i=1}^{N} \sigma_i^2)$ . These selected singular vectors  $(\mathbf{U}_s)$  form a basis for the observation data. Now, we construct an orthogonal projection matrix to the noise space as  $\mathbf{P}^{\perp} = \mathbf{I}_{N \times N} - \mathbf{U}_{s} \mathbf{U}_{s}^{T}$ . Using this matrix the MUSIC cost function is written as:

$$\alpha_i = \frac{\|\mathbf{P}^\perp \mathbf{a}_i\|_2^2}{\|\mathbf{a}_i\|_2^2},\tag{11}$$

where  $\mathbf{a}_i$  is the  $i^{th}$  columns in  $\mathbf{A}$ . Now a similar method to the step 3 in Section II-A is used to estimate the number of silences  $(\hat{k})$  based on the knee point in  $\tilde{\alpha}_i$  vs. i curve, where  $\tilde{\alpha}$  is the  $\alpha$  value sorted in descending order. Finally, Step 4 to 6 in Section II-A are repeated for this modified MUSIC algorithm to localize the silences, with using  $\alpha$  values instead of  $\beta_q$ . The selected sources in this algorithm are considered as silences since they have the minimum contribution in the observation matrix  $\mathbf{M}$ .

## III. RESULTS

In this section, we present the results of the proposed silence localization algorithm. In addition, we compare the performance of our algorithm with the classical source localization methods discussed in Section II.

We use the OASIS34 headmodel extracted from the MRI scan, as explained in Section I-A and simulate the source signals (S) based on assumptions in Section I-B. We create the region of silence in S by means of selecting a random

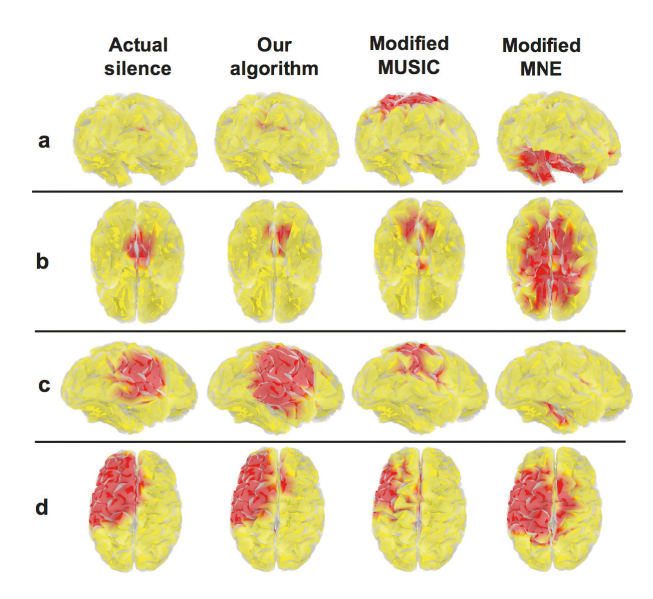


Fig. 2. Performance of our proposed algorithm in silence localization in comparison with classical source localization methods, i.e., modified MUSIC and MNE. Regions of silence (shown in red) are simulated at different parts of a real brain model, extracted from OASIS34 MRI scan: a) Single silence (k = 1), b) k = 50, c) k = 100, and d) k = 250.

source location in the brain and assigning silences to the k nearest neighbors. Observation data matrix (**M**) is obtained using (1). Here, we use a forward model with p = 1011, n = 44, and t = 10000. The noise variance ( $\sigma_n^2$ ) is chosen to make the minimum signal-to-noise-ratio (SNR) of the observation data equal to 2dB in these simulations. In addition, the threshold  $\gamma = 0.9$  is used in (8), which is found heuristically. This threshold depends on the orientation of column vectors of the forward matrix and can vary for different headmodels.

In our simulations, different numbers of silences are used to test the performance of silence localizations for both small and large regions of silences. Fig. 2 shows the results of silence localization for single silence source (k=1), small regions of silence (k=50) and 100, and a large region of silence (k=250). Based on these results, MUSIC fails to detect small regions of silence, and MNE fails to detect the region of silence for  $k \le 100$ . Our proposed algorithm performs significantly better in the detection of regions of silence for all values of k, compared to MNE and MUSIC.

In order to compare the performance of our proposed algorithm with MUSIC and MNE, the spatial bias in the localization of the region of silence is calculated for k=1. This spatial bias is the distance between geometrical central points of detected and actual regions of silence, averaged over trials. The number of trials is 500 in our simulations. Results show that the proposed algorithm has the smallest bias (14 mm), in comparison with the modified MNE (62 mm) and MUSIC (58 mm). In this paper, a headmodel with the minimum inter-source distance of 3.4 mm is used. The proposed algorithm reduces bias by a factor of  $\sim$  4 over classical source localization algorithms, and preliminary experiments suggest that it has a false alarm rate of < 0.02. In addition, the square root of the mean squared errors (MSE) in the estimation of k for the proposed algorithm,

the modified MUSIC and, MNE algorithm are 0.4, 9.5, and 17.8 respectively with k = 1. While these statistics seem promising, these results are yet to be tested on real EEG signals.

These preliminary results suggest that EEG has potential to be used as a non-invasive method for localizing silences in the brain. However, the proposed algorithm has limitations, e.g., this algorithm fails to correctly detect silences at locations whose corresponding columns in **A** have large correlation coefficients with columns of neighbors. To overcome this issue, we tried using a "successive refinement" approach. Due to space limitations, we have included the details of this method in the online version of this paper in [16], where a full detailed discussion appears.

#### REFERENCES

- K. Kamnitsas, C. Ledig, V. FJ. Newcombe, J. P. Simpson, A. D. Kane, D. K. Menon, D. Rueckert, and B. Glocker. Efficient multi-scale 3D CNN with fully connected CRF for accurate brain lesion segmentation. *Medical image analysis*, 36:61–78, 2017.
- [2] J. P. Dreier et al. Delayed ischaemic neurological deficits after subarachnoid haemorrhage are associated with clusters of spreading depolarizations. *Brain*, 129(12):3224–3237, 2006.
- [3] A. Chamanzar, S. George, P. Venkatesh, M. Chamanzar, L. Shutter, J. Elmer, and P. Grover. An algorithm for automated, noninvasive detection of cortical spreading depolarizations based on EEG simulations. *IEEE Transactions on Biomedical Engineering*, 2018.
- [4] A. Chamanzar, S. George, P. Venkatesh, W. Ding, and P. Grover. Systematic and automated algorithms for detecting cortical spreading depolarizations using EEG and ECoG to improve TBI diagnosis and treatment. In *Brain Injury*, volume 31, page 990. Taylor & Francis, 2017.
- [5] L. H. Juang and M. N. Wu. MRI brain lesion image detection based on color-converted K-means clustering segmentation. *Measurement*, 43(7):941–949, 2010.
- [6] C. R. Gillebert, G. W. Humphreys, and D. Mantini. Automated delineation of stroke lesions using brain CT images. *NeuroImage: Clinical*, 4:540–548, 2014.
- [7] B. A. Hargreaves, P. W. Worters, K. B. Pauly, J. M. Pauly, K. M. Koch, and G. E. Gold. Metal-induced artifacts in MRI. *American Journal of Roentgenology*, 197(3):547–555, 2011.
- [8] R. Srinivasan, D. M. Tucker, and M. Murias. Estimating the spatial Nyquist of the human EEG. *Behavior Research Methods, Instruments*, & Computers, 30(1):8–19, 1998.
- [9] P. L. Nunez and R. Srinivasan. Electric fields of the brain: the neurophysics of EEG. Oxford University Press, USA, 2006.
- [10] S. Baillet, J. C. Mosher, and R. M. Leahy. Electromagnetic brain mapping. *IEEE Signal processing magazine*, 18(6):14–30, 2001.
- [11] Y. Zhang, W. Van Drongelen, and B. He. Estimation of in vivo brain-to-skull conductivity ratio in humans. *Applied physics letters*, 89(22):223903, 2006.
- [12] R. Oostenveld, P. Fries, E. Maris, and J. M. Schoffelen. FieldTrip: open source software for advanced analysis of MEG, EEG, and invasive electrophysiological data. *Computational intelligence and neuroscience*, 2011:1, 2011.
- [13] B. Jeffs, R. Leahy, and M. Singh. An evaluation of methods for neuromagnetic image reconstruction. *IEEE Transactions on Biomedical Engineering*, (9):713–723, 1987.
- [14] V. Satopaa, J. Albrecht, D. Irwin, and B. Raghavan. Finding a "Kneedle" in a Haystack: Detecting Knee Points in System Behavior. In 2011 31st International Conference on Distributed Computing Systems Workshops, pages 166–171, June 2011.
- [15] M. Antunes, D. Gomes, and R. L. Aguiar. Knee/Elbow Estimation Based on First Derivative Threshold. In 2018 IEEE Fourth International Conference on Big Data Computing Service and Applications (BigDataService), pages 237–240, March 2018.
- [16] A. Chamanzar and P. Grover. Silence localization. https://cmu. box.com/s/jqdv17xjj2ozne43w8ib2mst3wge0n1c, 2018.